Neutron Scattering from Disordered and Fractal Magnets

Hironobu Ikeda

Booster Synchrotron Utilization Facility,

National Laboratory for High Energy Physics,

Oho 1-1, Tsukuba 305, Japan

Abstract

Over a period of twenty years, studies concerning disordered magnets, in which transition metals are considered to carry magnetic moments, have been performed using neutron-scattering techniques. This research field has been rich for testing theories of phase transitions and excitations in random magnetic systems; neutron experiments continue to provide crucial tests of theories and new challenges for theoretical work. We describe recent neutron-scattering studies on these system, which reveal the properties of the excitations and phase transitions of disordered systems. Special attention is paid to the very recent neutron-scattering studies on percolating magnets with a fractal geometry.

1 Introduction

In recent years random or disordered magnetic systems have attracted great interest among theoretical and experimental physicists. These are spin glasses, amorphous magnets, diluted magnets, random-field magnets, mixed antiferromagnets with two different magnetic species, and random systems of two magnetic species with competing spin anisotropies. In all these problems neutron scattering has played an important role, since from observations of the scattering function, which is the space-time Fourier transform of the spin pair-correlation function, one can obtain detailed information concerning the structural and dynamical properties of these systems, such as the order parameter, critical fluctuations, collective or localized magnetic excitations and diffusive spin motions.

Very recently, much attention has been paid to the static and dynamical properties of diluted magnets, whose magnetic concentration is very close to the percolation concentration. It is generally accepted that the atomic connectivity of a percolating cluster takes the form of a fractal (Stanley, 1977). The theory of

percolation has been formulated by many authors, and can now be used to interpret an exceptionally wide variety of physical and chemical phenomena, such as the gelation process (de Gennes, 1979), transport in amorphous materials (Zallen, 1983), and hopping conduction in a doped semiconductor (Shklovskii and Efros, 1984). The concept of fractals has contributed significantly to our understanding of percolation (Nakayama et al., 1994). The simplest ideal percolating networks are realized by substitutionally diluting magnetic systems by non-magnetic atoms. At a critical magnetic concentration c_p, a single infinite cluster (a percolating network) spans the full space; with a further decreasing concentration of magnetic atoms, the system splits into an assembly of only finite clusters. The percolating networks exhibit a self-similarity, and can be characterized by a non-integer mass dimension, i.e., a fractal dimension D_f. In a square and a simple cubic lattice, it has been numerically estimated that the D_f of the percolating network is 1.896 and 2.48 respectively, i.e., D_f is less than the Euclidian dimension D (Nakayama et al., 1994).

In this report, we present recent results concerning neutron-scattering experiments on two- and three-dimensional (2D and 3D) percolating antiferromagnets: a direct observation of the self-similarity of the magnetic order in a percolating cluster (Ikeda et al., 1993), and investigations of the magnetic fracton excitations in a percolating Heisenberg antiferromagnet (Ikeda et al., 1994), the observation of anomalous spin diffusion in a percolating cluster (Ikeda et al., 1995), and the observation of the ordering kinetics in a percolating Ising antiferromagnet (Ikeda et al., 1990).

2 Fractal structure and magnetic Bragg scattering

The scattering law for the fractal structure, which is observed by neutrons or photons, is quite simple. The small-angle neutron scattering intensity $I(q)$ is simply proportional to q^{-D_f}, where q is the wave vector. This relationship was actually observed by small-angle neutron scattering from silica aerogels (Vacher et al., 1988). However, an experimental observation of the self-similarity of the percolating network in diluted magnets was successful only recently.

Very recently, we achieved the first experimental observation of the fractal structure in diluted antiferromagnets (Ikeda et al., 1994). In the vicinity of the percolation threshold, the geometrical correlation length ξ_G is defined as $\xi_G = a_0 \mid c - c_p \mid^{-\nu_G}$, where ν_G is a numerical constant which depends on the lattice shape, and a_0 is the nearest-neighbour lattice spacing. It is now believed that this system is a fractal at length scales smaller than ξ_G; conversely, the system appears to be homogeneous at length scales larger than ξ_G. The geometrical corre-

lation length ξ_G is related to the crossover wave vector by $q_c = \xi_G^{-1}$. The systems in which the magnetic concentration c is very close to, or just above, the percolation threshold, order antiferromagnetically at low temperatures. The magnetic elastic scattering of neutrons from an infinite cluster in these systems, at the antiferromagnetic superlattice position, can be written as: $I(q) \propto \delta(\mathbf{Q} - \boldsymbol{\tau})$ for $q < q_c$, and $I(q) \propto q^{-D_f}$ for $q > q_c$; here, $\mathbf{q} = \mathbf{Q} - \boldsymbol{\tau}$, and $\mathbf{Q}$ and $\boldsymbol{\tau}$ are the scattering vector and the antiferromagnetic reciprocal vector, respectively. Below the transition temperature, spins belonging to the infinite network order magnetically, while those belonging to only finite clusters do not order, even at 0 K. It is important to note that magnetic correlations between an infinite cluster and finite clusters are absent due to a lack of magnetic interactions between them. This makes possible an observation of the fractal structure of an infinite cluster by a high-resolution measurement of the elastic-scattering profile near to the magnetic reciprocal point.

Our experiments were performed on a 2D diluted Ising antiferromagnet $Rb_2Co_cMg_{1-c}F_4$ ($c = 0.60$), whose magnetic concentration (0.60) is very close to the percolation threshold of a square lattice (0.593). The pure Rb_2CoF_4 system becomes antiferromagnetic at $T_N = 102.96$ K with the spin direction along the c-direction and alternating in the basal c-plane (Hutchings et al., 1982). The magnetic-exchange interaction dominates within the plane and is limited to the nearest neighbours. The measured Néel temperature of a $c = 0.60$ sample was 20.0 K, and the observed rounding of the transition was less than 1 K; hence, variations in the Co concentration are within $0.599 < c < 0.601$. Using the value of ν_G (1.33) for a square lattice system we can estimate the geometrical correlation length $\xi_G \approx 730\ a_0$ for $c = 0.60$, which implies a crossover wave vector q_c of 3.1 $\times 10^{-4}\, 2\pi/a$, where a ($\sqrt{2}\, a_0$) is taken as the unit length of the [1 0 0] direction. This sample is then expected to reveal a crossover at q_c, from a homogeneous structure at low q to a self-similar fractal structure at large q. Neutron elastic scattering experiments were performed on a triple-axis spectrometer (T1-1) installed at the thermal-neutron beam guide of the JRR-3M reactor at JAERI, Tokai. This was used in the triple-axis operation mode with the energy transfer fixed at 0 meV and with pyrolytic graphite crystals used as both the monochromator and analyzer. Collimations were open-10′-10′-20′ with incident energies of 13.7 meV. Higher-order contamination was eliminated by using a pyrolytic graphite filter. The crystal was oriented with its [0 0 1] axis vertical; the magnetic elastic scattering as a function of the wave vector along the [1 0 0] direction was measured at the (1 0 0) magnetic reciprocal position. The momentum-resolution width along the [1 0 0] direction was 0.0095 $2\pi/a$ at the full width at half maximum (FWHM). The scattered intensities $I(q)$ were corrected for a small, but constant, instrumental background.

Figure 1 shows the magnetic intensity distribution (plotted in a semi-logarithmic scale) measured from $Rb_2Co_{0.60}Mg_{0.40}F_4$. The intensity is shown as a function of

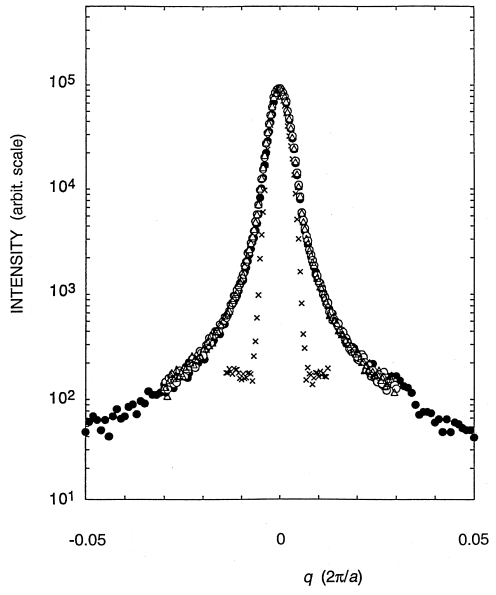

Figure 1. Scattered neutron intensities for $Rb_2Co_{0.60}Mg_{0.40}F_4$ near to the (1 0 0) antiferromagnetic reciprocal position measured at 4.5 K (solid circles), 7.5 K (open circles), 10 K (triangles) together with the instrumental resolution (crosses) in a semi-logarithmic plot.

q at $T = 7.5$ K (open circles) together with the instrumental resolution function (crosses). Below the transition temperature ($T_N = 20$ K) of this sample, three kinds of scattering contribute to the observed intensity. One is from the ordered pattern of the infinite network; the others are both from the critical magnetic fluctuations in an infinite cluster and thermal fluctuations in finite clusters. The line shape of the former is independent of the temperature, and takes the form of a δ-function if the system is homogeneous. The latter contribution is strongly temperature dependent with regard to both the intensity and the line width, as is well established. The absence of a temperature dependence in the scattering well below T_N (data at 4.5, 7.5 and 10 K in Fig. 1) indicates that the measured intensity is only from the ordered magnetic structure. This is due to the fact that the critical scattering in a 2D Ising system decreases very rapidly with decreasing temperature, and is clearly negligible at these temperatures. A remarkable feature of the line shape observed in the near-percolating system, $Rb_2Co_{0.60}Mg_{0.40}F_4$, is the very large width of the peak. This should be compared with the intrinsic δ-function peak arising from the antiferromagnetic long-range order (LRO) convoluted by the Gaussian resolution function (crosses in Fig. 1).

The data taken at 7.5 K were plotted in a double-logarithmic scale. The slope of the observed intensity versus the wave vector at $q > 0.01\ 2\pi/a$ is 1.95 ± 0.07. This value is in good agreement with the fractal dimension ($D_f = 1.896$) of an infinite cluster in a 2D percolating network. In the $c = 0.60$ sample, since the length scale expands to 730 a_0, a very large intensity from the self-similar fractal structure is observed over a large q region, as shown in Fig. 1. At q less than 0.005 $2\pi/a$, the Gaussian peak shape due to the magnetic long-range order is evident. Crossover from a homogeneous structure at small q to a fractal structure at large q is clearly seen in this figure. From similar experiments with different magnetic concentrations, we observed that the q values at which the scattering deviates from the Gaussian shape increases with increasing Co concentration. The observed crossover region in each sample with different concentrations is consistent with the estimated value of q_c mentioned earlier. This provides the first direct experimental observation of the self-similar structure of an infinite cluster in a diluted magnet close to the percolation threshold.

From the present experimental results we can directly conclude that the magnetic LRO below the second-order phase transition temperature is not always described by a δ-functional form in reciprocal lattice space. The self-similar fractal structure can be observed within a reasonable length scale in the simplest physical realization of a fractal system: a diluted antiferromagnet close to the percolation threshold.

3 Fracton excitations in a Heisenberg antiferromagnet

In recent years, considerable attention has been directed towards the dynamical properties of highly ramified percolating networks that exhibit a fractal geometry (Orbach, 1986). Recent theories and computer simulations of these systems predict the existence of highly localized fracton excitations with huge oscillation amplitudes (Alexander and Orbach 1982; Nakayama et al., 1994). A random site-diluted Heisenberg antiferromagnet is an ideal system for probing the existence of these excitations. In such a system and at concentrations close to, but just above, the percolation threshold there should be a crossover from long-wavelength spin-wave excitations to short-wavelength fracton excitations. The origin of this crossover is the fact that the fractal geometry is realized only at length scales shorter than the geometrical correlation length ξ_G (Stauffer, 1979). Magnetic excitations in diluted magnetic systems have been extensively studied using neutron inelastic scattering techniques (Cowley, 1981). However, a renewed experimental effort has recently been initiated to characterize the fractal component of the dynamics in these di-

luted magnetic systems. For this, it is important to distinguish fracton excitations from other localized excitations, such as Ising-like cluster excitations.

We have recently performed an experiment aimed to give the first quantitative measurement of fracton excitations in near-percolating Heisenberg systems (Ikeda et al., 1994). For this experiment we have chosen a diluted pure-Heisenberg antiferromagnet ($RbMn_{0.39}Mg_{0.61}F_3$), in which the Mn concentration (0.39) is very close to the percolation threshold ($c_p = 0.312$). The corresponding cross-over wave vector is $q_c = \xi_G^{-1} = 0.024$ reciprocal lattice units (rlu). The excitations with wave vectors smaller than q_c are expected to be spin waves, while the excitations with wave vectors larger than q_c are expected to be fractons. Since q_c in the present system is very small, the fracton region is observable in such an experiment.

Our experiment was performed on a single crystal (about 1 cm^3 in volume) of $RbMn_{0.39}Mg_{0.61}F_3$. The pure system $RbMnF_3$ has a cubic perovskite structure and becomes antiferromagnetic at $T_N = 82$ K with the spin directions alternating along the cubic edges. The $RbMn_{0.39}Mg_{0.61}F_3$ sample orders at 18 ± 1 K with the same magnetic configuration as in the pure system. The inelastic scattering measurements were performed on a triple-axis spectrometer installed at the HFIR reactor at the Oak Ridge National Laboratory (ORNL). The crystal was oriented with its [0 1 -1] axis vertical. The magnetic excitations were measured for wave vectors along the [0 1 1] direction from the $(\frac{1}{2}\ \frac{1}{2}\ \frac{1}{2})$ zone center ($q = 0$), to the zone boundary ($q = 0.375$ rlu).

Figure 2 shows the energy spectrum of the magnetic response, taken at 4.5 K, at the zone boundary corrected for instrumental background. As depicted in the figure, a fine structure due to the Ising-cluster excitations in this system appears. The vertical bars in the figure give the probability density of random populations of magnetic neighbors for $c = 0.39$. The energy values at the peaks agree with the Ising-cluster energies of Mn^{2+} ions when an exchange constant of $J = 0.30$ meV is used. No measurable intensity is expected at the highest position of 9.0 meV ($z = 6$) due to the small probability for 6 magnetic neighbors. It should be noted, however, that the observed magnetic response extends beyond 8 meV where no magnetic intensities from the cluster excitations are expected. This observation indicates that the energy spectrum at the zone boundary, in this system, cannot be described solely by a simple Ising-cluster model. Since the energy resolution (1.0 meV FWHM) is finer than the peak interval (1.5 meV), the contribution from the cluster excitations can be resolved from the additional magnetic scattering. This additional magnetic contribution is indicated by the dotted line in Fig. 2.

The energy spectra obtained at several wave vectors from $q = 0$ to 0.375 rlu (ZB) reveal that the observed line shapes are not smooth, but have some small structure, originating from the cluster excitations, throughout the Brillouin zone. Also, over the entire Brillouin zone the energy spectrum of the additional contribution shows

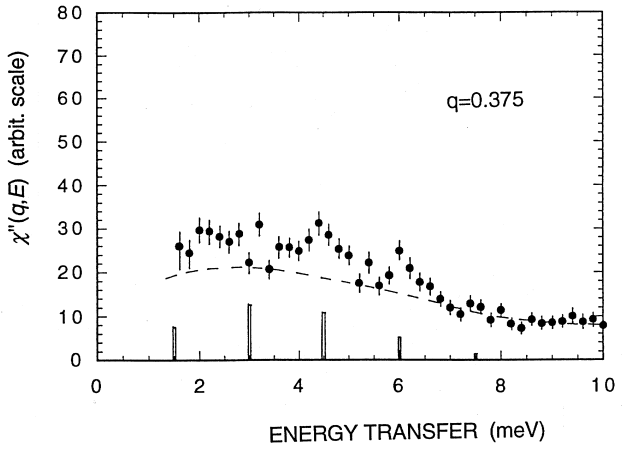

Figure 2. Magnetic response $\chi''(q, E)$ of $RbMn_{0.39}Mg_{0.61}F_3$ observed at the zone boundary at 4.5 K with an energy resolution of 1.0 meV. The vertical bars indicate the probability density of random populations of magnetic neighbours. The dotted line represents the additional magnetic contribution and also the fitted scattering function described in the text. Vertical bars represent error bars.

a very broad, smooth shape, and its magnetic response extends to the highest energies measured in our experiment (10 meV). The energy width of this spectrum is much broader than the energy resolution. As the wave vector increases, the intensity of the scattered neutrons decreases rapidly.

We have analysed the line shape of the magnetic response of an additional magnetic contribution obtained at 4.5 K. From a physical point of view, a damped harmonic oscillator (DHO) would be the most reasonable model to fit these excitations. We therefore fitted the broad excitation data to the functional form $\chi''(q, E) = A\Gamma(q)E/[(E^2 - E_p(q)^2)^2 + (\Gamma(q)E)^2]$, where A is a constant. This form was successfully fitted to all of the data. The fitted values of $E_p(q)$ and $\Gamma(q)$ as a function of q satisfy the power-law relationship with the same exponent, i.e., $E_p(q) \propto \Gamma(q) \propto q^{1.1\pm0.2}$. It should be noted that since the value of $\Gamma(q)$ is much larger than $E_p(q)$, the excitations are strongly over-damped over the entire Brillouin zone. It has been recently reported that the single length-scale postulate (SLSP) holds for the magnetic response from fractons (Nakayama et al., 1994). This postulate states that the peak energy and the energy width should have the same wave-number dependence as q^{z_a}, i.e., $E_p(q) \propto \Gamma(q) \propto q^{z_a}$. The present result is in accord with this theory.

A similar analysis using a DHO form has been performed in the nearly perco-

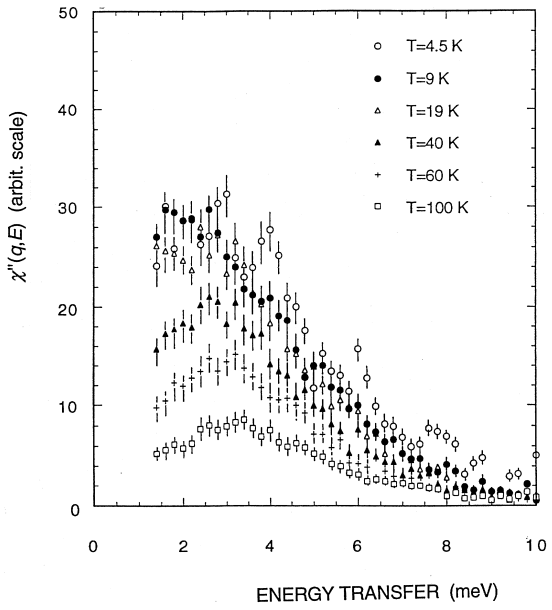

Figure 3. Temperature variation of $\chi''(q, E)$ at $q = 0.2$ as a function of energy transfer observed at $T = 4.5$ K (open circles), 9 K (closed circles), 19 K (open triangles), 40 K (closed triangles), 60 K (crosses) and 100 K (open squares). Vertical bars represent error bars.

lating antiferromagnet $Mn_{0.32}Zn_{0.68}F_2$ by Coombs et al. (1976). We presume that their over-damped signal might have contained contributions from both fracton and Ising-cluster excitations, although a separation of these was not pursued.

Another evidence for fractons is seen in the temperature variation of $\chi''(q, E)$ at wave vectors larger than q_c. In Fig. 3, the energy spectra at $q = 0.2$ rlu obtained from $T = 9$ K to 100 K are shown. At $T = 9$ K ($T_N/2$), peaks from Ising-cluster excitations almost disappear due to the much more enhanced thermal fluctuations of the molecular fields than at $T = 4.5$ K. On the other hand, the over-damped component is predominant at this temperature, and the line shape is the same as that measured at $T = 4.5$ K. In this figure we observe the remarkable fact that the over-damped component can survive even at $T = 100$ K ($> 5\ T_N$), and the peak energy slightly shifts towards higher energies with increasing T. These are completely different from the traditional spin-wave excitations in the Heisenberg system. The increase in the peak energy could be related to the localized nature of fractons, and thus the excitation energy (oscillating frequency) could be increased by obtaining the thermal energy.

On the other hand, high-resolution inelastic neutron-scattering studies have recently been performed on a three-dimensional (3D) diluted near-Heisenberg antiferromagnet ($Mn_{0.5}Zn_{0.5}F_2$) by Uemura and Birgeneau (1986, 1987). They ascribed the asymmetry of the obtained spectra and the double-peak structure at small wave vectors to the coexistence of magnons and fractons, and its wave-vector dependence to the magnon-fracton crossover. This interpretation should be taken with caution, however, because the magnetic concentration of the system that they studied (0.5) is far above the percolation threshold ($c_p = 0.245$ or less for a body-centered tetragonal lattice). At this relatively high magnetic concentration it is difficult to obtain conclusive evidence of fractons, since the system is not self-similar, even at small length-scales.

Our arguments, based on the DHO function, are qualitatively in good agreement with the current theory for fractons, although a quantitative description of the physical properties of the antiferromagnetic fractons in a Heisenberg system has not yet been completely resolved. We hope that an accurate description, even for the magnetic response function itself, will be available in the near future from analytic theories and/or computer simulations.

4 Anomalous diffusion and self-correlation function

The observation of a single-spin diffusive motion on a percolating network having fractal geometry has been a long-standing problem concerning the dynamical properties of percolation (Aeppli et al., 1984). In uniform systems, the mean-square displacement of a random walker $\langle R^2(t)\rangle$ is proportional to the time t, $\langle R^2(t)\rangle \propto t$, for any Euclidean dimension. In percolating systems with fractal geometry, the diffusion is anomalous, and the mean-square displacement is described by $\langle R^2(t)\rangle \propto t^{2/(2+\Theta)}$ ($\Theta > 0$) (Gefen et al., 1983). Here, Θ is defined using the critical exponents β, ν and μ, where β describes the probability of a site belonging to the infinite network and ν and μ represents the average size and the average mass (number of sites) of finite clusters as a function of the concentration, respectively. These exponents were numerically estimated and for a 2D system Θ is 0.871 (Havlin and Bunde, 1991). This causes a slowing down of the diffusion of a spin due to the irregular path-structure of a fractal.

In order to observe anomalous spin diffusion using neutron scattering, the following considerations were made: (1) The diffusion of spins on percolating networks can be observed by neutron magnetic scattering. (2) Slow diffusion requires a very high energy-resolution, particularly in a 2D system. (3) An observation of the self-correlation function $\langle S_0(0)S_0(t)\rangle$ (where the subscript 0 refers to the

lattice site) is essential for studying anomalous diffusion due to the single-spin nature of motions. This quantity is inversely proportional to the volume $V(t)$ which can be occupied by a single spin during time t. That is, $\langle S_0(0)S_0(t)\rangle \propto V(t)^{-1} \propto R(t)^{-D_f} \propto t^{-D_f/(2+\Theta)}$, where D_f is the fractal dimension; for a square-lattice system it has been numerically estimated that D_f of a percolating network is 1.896. A Fourier transform of this quantity gives the following relationship: $S(E) = \int \langle S_0(0)S_0(t)\rangle\, e^{-iEt}\, dt \propto E^{D_f/(2+\Theta)-1}$. This quantity is obtained by integrating the generalized scattering function $S(q, E)$ over q. (4) Since $D_f/(2+\Theta) - 1 = -0.34$ the form of $S(E)$ exhibits a long tail, which makes it distinguishable from the tail of the Lorentzian lineshape, which is typical for critical magnetic scattering.

Neutron inelastic-scattering experiments were performed using the IRIS spectrometer at the ISIS pulsed spallation neutron source in Rutherford Appleton Laboratory (RAL), UK (Ikeda et al., 1995). IRIS is an inverted geometry spectrometer in which the neutrons scattered from the sample are energy-analyzed by being Bragg diffracted by large-area arrays of single crystals of mica and pyrolytic graphite (Carlile and Adams, 1992). For the experiment detailed here the (0 0 4) reflection of the mica analyzer bank was used with an energy resolution of 4 μeV and a fixed final energy of 0.832 meV. The mica detector bank has 51 separate elements covering a 2θ-range of 25° to 155°. Inelastic signals can thus be observed simultaneously over a wide-range of momentum transfer with a high energy-resolution. The energy-transfer range covered in these experiments was −0.15 meV (neutron energy gain) to +0.15 meV (neutron energy loss).

The sample used in the present experiments was a 2D square-lattice antiferromagnetic insulator diluted by non-magnetic Mg atoms, $Rb_2Co_{0.6}Mg_{0.4}F_4$. The spins ($S = 1/2$) in the material are localized, and it is the diffusion which is observed. The Co concentration is very close to, but slightly above, the percolation threshold (0.593). The magnetic-exchange interaction dominates within the plane, and is limited to the nearest neighbors. A large single-crystal (diameter 30 mm and height 12 mm) sample of $Rb_2Co_{0.6}Mg_{0.4}F_4$ having a cylindrical shape was successfully grown using the Bridgman method. The c axis coincides exactly with the cylindrical axis. The Néel temperature T_N measured with a magnetic susceptometer was 17.0 ± 0.2 K, and no appreciable rounding of the transition was observed. The mosaic spread of the sample was less than 0.5°. Lattice constants a_0 and c_0 were 5.78 and 13.71 at $T = 5$ K, respectively.

The sample was mounted in a liquid-helium cryostat with its c axis vertical to the neutron scattering plane. The detectors at 2θ-angles between 68.8° and 145.5° were used for integrating the intensity $S(q, E)$ over the momentum. These detectors covered a wide momentum space centered at the (1 0 0) magnetic reciprocal point. No magnetic scattering was observed in the other detectors, at any tem-

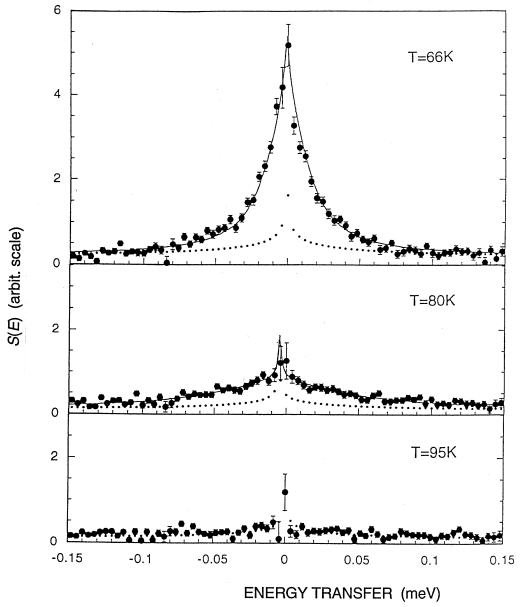

Figure 4. Self-correlation function $S(E)$ of $Rb_2Co_{0.6}Mg_{0.4}F_4$ as a function of the energy transfer observed at 66, 80 and 95 K. The solid lines indicate the results of a fit to the sum of the Lorentzian and $E^{-0.35}$ form. The dotted lines represent the contribution from only the $E^{-0.35}$ form. The vertical bars represent error bars.

perature measured, because these detectors viewed a region of momentum space well away from the magnetic reciprocal lattice point. Effectively, each detector element was associated with an area of the mica analyzer of dimensions 30 mm wide and 200 mm high. The large height of the analyzer provided a high counting rate without compromising the momentum resolution, because the 2D nature of the sample means that the momentum transfer in the vertical direction at a particular scattering angle 2θ, is identical.

Experiments were performed at several temperatures above and below T_N. Figure 4 shows the self-correlation function as a function of the energy-transfer, measured at $T = 66$, 80 and 95 K. As depicted, a long-tailed spectrum extending towards a high energy-transfer is clearly observed. The overall spectrum is quite different from the lineshape of the critical magnetic scattering. Fitting the data with a Lorentzian lineshape was of course not successful. Since the system has a Néel temperature of 17 K, strong critical scattering with a Lorentzian lineshape is expected; we therefore fitted the data with the sum of the Lorentzian and E^{-x}-form. The best result was obtained with x being between 0.3 and 0.4

($x = 0.35 \pm 0.06$), suggesting that the long-E tail comes from anomalous diffusion, which predicts the $E^{-0.34}$-form in the scattering function. The best results of a fitting with $x = 0.35$ are shown by the solid lines in Fig. 4, where the dotted lines describe the contribution from only $E^{-0.35}$. This fitting was successful for all of the data taken above and below T_N. Although the fitting to the sum of two functional forms is successful at any temperature, on approaching T_N the critical scattering is more dominant, as was expected. On approaching T_N, the thermal correlation length becomes large, and the picture of single-spin diffusion does not hold. This causes the decrease in amplitude of $E^{-0.35}$ near to T_N.

This experiment provides evidence for the anomalous diffusive motions of spins in a near-percolating Ising antiferromagnet, $Rb_2Co_{0.6}Mg_{0.4}F_4$. The scattering function integrated over momentum space in the paramagnetic phase reveals a long-tailed spectrum with the form of $E^{-(0.35\pm0.06)}$ superimposed on the Lorentzian lineshape, which originates from the normal critical magnetic scattering.

5 Ordering kinetics in fractal networks

The ordering kinetics of a pure Ising model with a nonconserved order parameter has been extensively studied both theoretically and experimentally (Gunton et al., 1983). The order develops from the initial disordered state to the final long-range ordered (LRO) state after rapid quenching from a high-temperature paramagnetic state to an ordered state below its transition temperature. Theories as well as computer simulations and experimental observations in metallic binary alloys have proved that the temporal development of the order obeys $t^{1/2}$ law during the last stage. However, it has been unclear how the order develops in a highly diluted magnet in which the magnetic concentration is close to the percolation threshold; the ordered cluster is therefore highly ramified and takes the form of a fractal. We have recently succeeded in observing the ordering kinetics of a highly diluted antiferromagnet, $Rb_2Co_{0.60}Mg_{0.40}F_4$, with a fractal geometry by both neutron elastic scattering and magnetization measurements (Ikeda et al., 1990).

In order to observe how a system develops in going from a disordered initial state to a final LRO state, one may cool the sample very rapidly from a high-temperature paramagnetic state to an ordered state at low temperature. In magnetic substances, however, the LRO is quickly stabilized when passing through the phase transition temperature and, hence, it was too difficult to observe a temporal growth of the domain size on a real time scale. In the present experiments, we utilized a new idea to realize the initial disordered state. As has been extensively argued during the last decade, the LRO in 2D diluted Ising antiferromagnets is destroyed by a uniform magnetic field applied along the spin direction and the

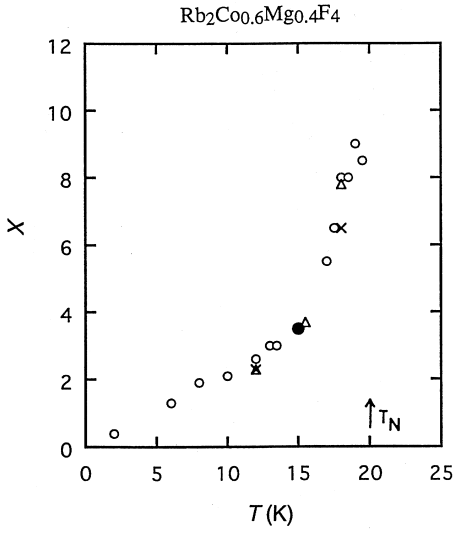

Figure 5. x versus T for data taken with external field cooling of 1 tesla (open circles), 2 tesla (triangles), and 3 tesla (crosses). x was found from fits of the magnetization by $[\log_{10}(t)]^{-x}$. The neutron data point is denoted by the solid circle.

system is broken into a micro-domain state (random-field effect) (Birgeneau et al., 1984; Belanger 1988; Nattermann and Villain, 1988). Experiments have verified that the equilibrium domain size in an external field decreases with increasing field and with decreasing magnetic concentration. Our observation of the equilibrium domain size of $Rb_2Co_{0.60}Mg_{0.40}F_4$ in a field of 4.8 tesla showed only 12 a_0. This value is actually microscopic. Furthermore, we found that after removing the field the LRO recovers within a macroscopic time scale, typically from several hours to several days. These facts have enabled us to observe the ordering kinetics on a real time scale.

For the time-resolved experiments, we performed both neutron-scattering and magnetization measurements. In both pure and diluted antiferromagnets, a system having a LRO has no net magnetization at all. However, in a cluster having a finite size a ferromagnetic moment arises along the magnetic field due to a statistical excess of the number of up-spins. Simple argument gives rise to a relationship between the micro-domain size R and the induced ferromagnetic moment M as $R \propto 1/M$, even in a system with fractal geometry. Therefore, the temporal decrease in $M(t)$ corresponds to the time evolution of the domain size $R(t)$.

For magnetization measurements a small piece of 0.0550 g mass was cut out of the single crystal and mounted in a SQUID susceptometer. The crystal was

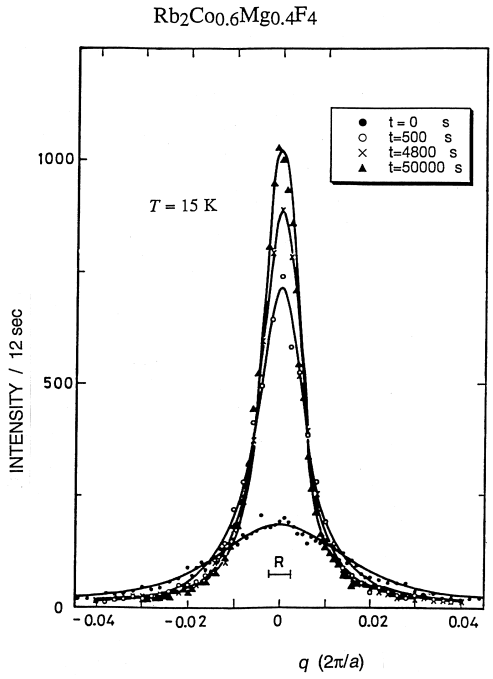

Figure 6. Temporal variation of transverse scans across the (1 0 0) superlattice position at $T = 15$ K; the cooling field was 4.8 tesla. The solid lines represent fit by a single Lorentzian convoluted with the instrumental resolution function. R represents the resolution width.

cooled down to several designated temperatures below T_N (20 K) while an external magnetic field was applied along the c axis. The applied field was turned off after reaching the desired temperature and the magnetization measurement was performed in a zero field. The temporal decay rate of the magnetization is clearly temperature dependent. This suggests that the growth rate of the order is governed by thermally activated magnetic fluctuations. In order to analyze the magnetization data, we made fits with several different functional forms, including a simple power law; in the end, however, we obtained the best results using a logarithmic power law, $M(t)^{-1} = A + B[\log_{10}(t)]^x$, where A, B, and x are adjustable parameters. We plot x as a function of temperature in Fig. 5, where the results for 1 T, 2 T and 3 T cooling are depicted. Note that x goes to zero as T approaches zero, indicating that the kinetics are frozen at $T = 0$. This provides further support for our conjecture of thermally driven kinetics.

In order to directly observe the domain size as a function of time, neutron-

scattering experiments using a TUNS spectrometer installed at JRR-2, JAERI, were performed. We used a triple-axis mode of operation with the transferred energy fixed at zero using incident neutron of 13.7 meV. An external field up to 5 tesla in magnitude was applied in the vertical direction, so that the single crystal was mounted in a cryostat with the c axis (spin direction) vertical. In order to obtain the best instrumental resolution possible, transverse scans across the (1 0 0) superlattice Bragg point were performed. The resolution of the spectrometer under these conditions was typically 0.0050 FWHM in reciprocal lattice units (rlu) (1 rlu $= 2\pi/a = 1.097$ Å^{-1}). The time dependence of the line shape with the transverse scan was measured at 15 K for 4.8 T field cooling of the sample and was directly compared with the magnetization measurements. The scan was repeated over a period of 15 hours. Each scan takes approximately 15 min. Typical line shapes at different times are shown in Fig. 6. The line shape was fitted with several functions of the structure factor: a Lorentzian, a squared Lorentzian and the form $(\boldsymbol{\kappa}^2 + \mathbf{q}^2)^{-1.5}$. The sum of mean square deviations (χ^2) in the Lorentzian fitting for 62 scans is less than the other two. The average domain size as determined from fits by a single Lorentzian gives an exponent x of 3.5 at 15 K. This value is in good agreement with the magnetization result. From these results we found that in the above time intervals the observed domain size satisfies the self-similarity condition $R(t) < \xi_G$, where the geometrical correlation length ξ_G in the present sample is 730 a_0, and, therefore, large enough.

Although the logarithmic time dependence of the domain size $R(t)$ has been discussed in earlier theoretical works (Grest and Slorivitz, 1985: Slorovitz and Grest, 1985; Huse and Henley, 1985; Chawdhury et al., 1987), to the best of our knowledge this is the first experiment which actually shows the $\log(t)$ power-law behaviour and kinetics which exhibits freezing at $T = 0$.

In a magnet with quenched impurities, the impurities act as energy barriers to domain growth; the pinning walls are therefore localized in energetically favourable positions, drastically slowing down the ordering kinetics. In particular, freezing in the percolating magnets should involve domain motion, which should be dependent on R; in other words, the energy barrier is dependent on R: $E(R) = (1/F)(R - R_0)^{1/x}$ (Lai et al., 1988). Here, R_0 and F are only weakly temperature dependent. Since the time necessary to overcome such barriers will have an activated temperature dependence, $t \approx \tau_1 \exp[E(R)/T]$, the growth law for the domain size in this model will have a logarithmic dependence, $R(t) = R_0 + FT[\ln(t/\tau_1)]^x$. Our experiment shows that x is dependent on the temperature and that it drastically increases as the temperature approaches T_N (20 K). We believe that although this behaviour might be related to critical fluctuations, thermally controlled domain-wall motion dominates the ordering kinetics.

Acknowledgements

The author would like to thank many of his collaborators, K. Iwasa, S. Itoh, M. Takahashi, K.H. Andersen, J.A. Fernandez-Baca, R.M. Nicklow and M.A. Adams for their important contributions. Work at National Laboratory for High Energy Physics (KEK) waa supported by a Grant-in-Aid for Scientific Research from the Japanese Ministry of Education, Science, Sports and Culture. The work at RAL and ORNL was performed under the UK-Japan and US-Japan Collaboration Program in Neutron Scattering, respectively.

References

Aeppli G, Guggenheim HJ and Uemura YJ, 1984: Phys. Rev. Lett. **52**, 942
Alexander S and Orbach R, 1982: J. Phys. Lett. (Paris) **43**, L625
Belanger DP, 1988: Phase Transitions **11**, 53
Birgeneau RJ, Cowley RA, Shirane G and Yoshizawa H, 1984: J. Stat. Phys. **34**, 817
Carlile CJ and Adams MA, 1992: Physica B **182**, 431
Chawdhury D, Grant M and Gunton JD, 1987: Phys. Rev. B **35**, 6792
Coombs GJ, Cowley RA, Buyers WJL, Svensson EC, Holden TM and Jones DA, 1976: J. Phys. C **9**, 2167
Cowley RA, 1981: *Excitations in Disordered Systems*, ed. M.F. Thorpe (Plenum, New York)
de Gennes PG, 1979: *Scaling Concepts in Polymer Physics* (Cornell Univ. Press, Ithaca)
Gefen Y, Aharony A and Alexander S, 1983: Phys. Rev. Lett. **50**, 77
Grest GS and Slorovitz DJ, 1985: Phys. Rev. B **32**, 3014
Gunton JD, San Miguel M and Sahni PS, 1983: in *Phase Transitions and Critical Phenomena*, eds. C. Domb and J.L.L. Lebowitz (Academic, New York) Vol. 8
Havlin S and Bunde S, 1991: in *Fractals and Disordered Systems*, eds. A. Bunde and S. Havlin (Springer-Verlag, Berlin)
Huse DA and Henley CL, 1985: Phys. Rev. Lett. **54**, 2708
Hutchings MT, Ikeda H and Janke E, 1982: Phys. Rev. Lett. **49**, 86
Ikeda H, Endoh Y and Itoh S, 1990: Phys. Rev. Lett. **64**, 1266
Ikeda H, Iwasa K and Andersen KH, 1993: J. Phys. Soc. Jpn. **62**, 3832
Ikeda H, Fernandez-Baca JA, Nicklow RM, Takahashi M and Iwasa K, 1994: J. Phys. Condens. Matter **6**, 10543
Ikeda H, Itoh S and Adams MA, 1995: Phys. Rev. Lett. **75**, 4440
Lai Z, Mazenko GF and Valls OT, 1988: Phys. Rev. B **37**, 9481
Nakayama T, Yakubo K and Orbach R, 1994: Rev. Mod. Phys. **66**, 381
Nattermann T and Villain J, 1988: Phase Transitions **11**, 5
Orbach R, 1986: Science **251**, 814
Shklovskii BI and Efros AF, 1984: *Electronic Properties of Doped Semiconductors* (Springer-Verlag, Berlin)
Slorovitz DJ and Grest GS, 1985: Phys. Rev. B **32**, 3021
Stanley HE, 1977: J. Phys. A **10**, L211
Stauffer D, 1979: Phys. Rep. **54**, 2
Uemura YJ and Birgeneau RJ, 1986: Phys. Rev. Lett. **57**, 1947
Uemura YJ and Birgeneau RJ, 1987: Phys. Rev. B **36**, 7024
Vacher R, Woignier T, Pelois J and Courtens E, 1988: Phys. Rev. B **37**, 6500
Zallen R, 1983: *The Physics of Amorphous Solids* (John Wiley & Son, New York)